Scientific Research Publishing

Open Journal of Modern Hydrology, 2016, 6, 230-252
http://www.scirp.org/journal/ojmh
ISSN Online: 2163-0496
ISSN Print: 2163-0461

Application of the Reciprocal Analysis for Sensible and Latent Heat Fluxes with Evapotranspiration at a Humid Region

Toshisuke Maruyama*, Manabu Segawa

Faculty of Environmental Science, Ishikawa Prefectural University, Ishikawa, Japan
Email: *maruyama@ishikawa-pu.ac.jp, manabu@ishikawa-pu.ac.jp

How to cite this paper: Maruyama, T. and Segawa, M. (2016) Application of the Reciprocal Analysis for Sensible and Latent Heat Fluxes with Evapotranspiration at a Humid Region. *Open Journal of Modern Hydrology*, **6**, 230-252.
http://dx.doi.org/10.4236/ojmh.2016.64019

Received: August 17, 2016
Accepted: October 17, 2016
Published: October 20, 2016

Abstract

Evapotranspiration acts an important role in hydrologic cycle and water resources planning. But the estimation issue still remains until nowadays. This research attempts to make clear this problem by the following way. In a humid region, by applying the Bowen ratio concept and optimum procedure on the soil surface, sensible and latent heat fluxes are estimated using net radiation (*Rn*) and heat flux into the ground (*G*). The method uses air temperature and humidity at a single height by reciprocally determining the soil surface temperature (*Ts*) and the relative humidity (*rehs*). This feature can be remarkably extended to the utilization. The validity of the method is confirmed by comparing of observed and estimated latent (*lE*) and sensible heat flux (*H*) using the eddy covariance method. The hourly change of the *lE*, *H*, *Ts* and *rehs* on the soil surface, yearly change of *lE* and *H* and relationship of estimated *lE* and *H* versus observed are clarified. Furthermore, monthly evapotranspiration is estimated from the *lE*. The research was conducted using hourly data of FLUXNET at a site of Japan, three sites of the United States and two sites of Europe in humid regions having over 1000 mm of annual precipitation.

Keywords

Bowen Ratio, Eddy Covariance, Reciprocal Determination, Estimation of Sensible and Latent Heat Fluxes, Soil Surface Temperature and Humidity

1. Introduction

In the natural world, the air temperature and humidity are determined by *H* and *lE* from the net radiation (*Rn*) and heat flux into the ground (*G*). Therefore, our research attempts the reciprocal analysis of *H* and *lE* from the air temperature (*Tz*) and humidity

(*rehz*) at single height while satisfying the heat balance relationship. The concept can't find the other relevant methods, and it only requires *Rn*, *G*, *Tz* and *rehz*. This feature is remarkably widened a utilization purposes.

Recently, we reported the reciprocal analysis of sensible and latent heat fluxes in a forest region [1]. However, "humid region" is quite different from "forest region" because of no canopy. This paper described "humid region" instead of "forest region", although there was similar concept in previous research.

The main different point is: the present paper contains two unknown variables, *i.e.*, relative humidity (*rehs*) and temperature on the soil surface (*Ts*) while the previous paper contains only one variable, *i.e.*, *rehs*, on the canopy surface. Therefore, the analysis has differences in that the present paper has to solve two simultaneous equations while the previous paper solved only one equation. In the analytical process, various new points arisen. Addition, this paper describes the comparison of the Penman method with our method because of humid region.

In the proposed method, the unknown variables, *Ts* and *rehs* were determined by the non-linear optimization technique known as the general reduced gradient (GRG) using the Excel Solver (**Appendix 1**).

2. Materials

We proposed a general method for estimating sensible and latent heat flux using single height temperature and humidity. The method contains two unknown variables: soil surface temperature, *Ts*, and humidity, *rehs*. This chapter describes the theoretical background for estimating *Ts* and *rehs*, the practical procedure, data correction, the details of test sites and measurement instruments.

2.1. Method of Analysis

2.1.1. Fundamental Concept of the Model

A proposed model is somewhat similar to previous research [1]. Therefore, briefly the outline is described. The proposed model considers the near-soil surface as shown in **Figure 1**.

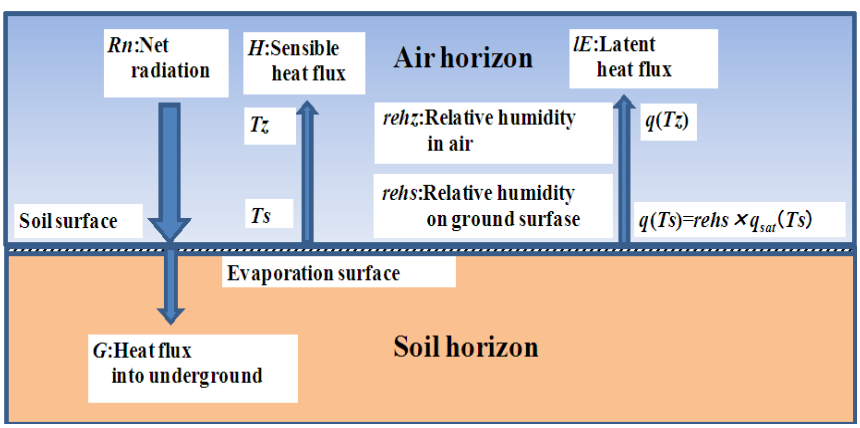

Figure 1. Components of the model and the relevant symbols.

Here, *Rn* is net radiation which is portioned into sensible, latent and underground heat fluxes. *Ts* is the soil surface temperature, *Tz* is the air temperature at height *z*, $q(Tz)$ is the specific moisture at height *z*, *rehz* is relative humidity in air at height *z*, $q(Ts)$ is the unsaturated specific moisture on the soil surface, and $q_{sat}(Ts)$ is the saturated specific moisture on the soil surface.

The fundamental formulae of the model satisfy the following well-known heat balance relationship [2].

$$Rn = H + lE + G. \tag{1}$$

Here, *Rn* is the net radiation flux (W·m^{-2}), *G* is the heat flux into the ground (W·m^{-2}), *H* is the sensible heat flux (W·m^{-2}), and *lE* is the latent heat flux (W·m^{-2}).

In addition, the Bowen ratio (*H*/*lE*) is defined as follows [2]:

$$B_0 = \frac{Cp(T_1 - T_2)}{l(q_1 - q_2)}. \tag{2}$$

We apply the concept of Bowen ratio to the layer between the soil surface and observation height of *Tz* and *rehz*. But, the *Ts* and $q(Ts)$ are just on the surface and usually unknown.

2.1.2. Governing Equation for Estimating the Unknown Variables *Ts* and *rehs*

The governing equation to be solved is obtained by heat balance relationship [1]. The unknown variables *Ts* and *rehs* are estimated as follows: The *Ts* and the $q(Ts)$, *i.e.*, *rehs* × e_{sat} (*Ts*) are assumed initially; thus, the heat balance relationship has not closed as Equation (3):

$$R_n - G - H_{est,i} - lE_{eat,i} = \varepsilon_i \quad i = 1, 2, 3, \cdots n \tag{3}$$

$$B_{app,i} = \frac{H_{est,i}}{lE_{est,i}} = \frac{Cp(T_{s,ass} - T_z)}{l\left[q(T_{s,ass}) - q(T_z)\right]} \tag{4}$$

$$lE_{est,i+1} = \frac{Rn - G}{1 + B_{app,i}} \quad \text{and} \quad H_{est,i+1} = B_{app,i} \times lE_{est,i+1}. \tag{5}$$

Here *i* is number of iteration. $H_{est,i}$ is estimated sensible heat flux in *i* times iteration, $lE_{est,i}$ is estimated latent heat flux, ε_i is residual of heat balance relationship of *i* times iteration, Ts_{ass} is assumed soil surface temperature, $q(Ts_{ass})$ is specific moisture at Ts_{ass}, B_{app} is apparent ratio of sensible and latent heat flux under convergence process.

The approximated *Ts* and *rehs* putting in Equation (4), *lE* and *H* of next order approximated values obtained by Equation (5).

By repeating the above calculation from Equation (3) to Equation (5), the B_{app} converged to B_0 according to objective function ABS (ε_i) conversed to a minimum.

After optimization, B_{app} is conversed to B_0. Then, lE_{est} and H_{est} can be obtained as follows:

$$lE_{est} = \frac{Rn - G}{1 + B_0} \quad \text{and} \quad H_{est} = B_0 \times lE_{est}. \tag{6}$$

To estimate *Ts*, an adjustment factor *RTs* was introduced using T_0 as follows:

$$T_s = G \times D_{To} / Kt \times RTs + T_0 . \quad (7)$$

Here, T_0 is the observed soil temperature (˚C), D_{To} is the depth of the temperature observation (cm), Kt is the assumed thermal conductivity (W·m^{-1}·˚C^{-1}).

Equation (7) describes how to obtained Ts by extrapolating T_0 using G, D_{To} and Kt. The calculation follows General Reduced Gradient (GRG) algorithm, which can be applied with the Excel Solver on a personal computer (Appendix 1 and Appendix 2).

2.1.3. General Solution

To uniquely determine the two unknown variable Ts and $rehs$, two equations are required mathematically. We set the two equations as follows assuming Ts and $rehs$ has no remarkable difference between two unit hours:

$$R_n^j - G^j - H_{est,i}^j - lE_{est,i}^j = \varepsilon_i^j \quad (8)$$

$$R_n^{j+1} - G^{j+1} - H_{est,i}^{j+1} - lE_{est,i}^{j+1} = \varepsilon_i^{j+1} . \quad (9)$$

Here, j is the order of hours from 1 to the end of the analyzed hours and i is the number of iterations.

The calculation is performed by solving Equation (8) and Equation (9) simultaneously under $T^j = Ts^{j+1}$ and $reh^j = rehs^{j+1}$ conditions: $\varepsilon = \mathrm{ABS}\left[\varepsilon_i^j\right] + \mathrm{ABS}\left[\varepsilon_i^{j+1}\right]$ conversed to minimum.

In addition, to prevent abnormal fluctuation of H_{est} versus lE_{est} in optimization process, constraints $Rn - G < H$, lE are applied as follows (Equation (10)):

$$\left.\begin{array}{l} \left\{\mathrm{ABS}\left(H^j\right) + \mathrm{ABS}\left(H^{j+1}\right)\right\} < \left\{\mathrm{ABS}\left(Rn^j - G^j\right) + \mathrm{ABS}\left(Rn^{j+1} - G^{j+1}\right)\right\} \mathrm{for} H \\ \left\{\mathrm{ABS}\left(lE^j\right) + \mathrm{ABS}\left(lE^{j+1}\right)\right\} < \left\{\mathrm{ABS}\left(Rn^j - G^j\right) + \mathrm{ABS}\left(Rn^{j+1} - G^{j+1}\right)\right\} \mathrm{for} lE \end{array}\right\} . \quad (10)$$

Equation (8) and Equation (9) are nonlinear two element simultaneous equations. The two unknown variables can be estimated for the limit to which ε is minimized, allowing H and lE to be estimated. Note that the other factors were obtained from observations or were calculated independently.

2.1.4. Correction of the Heat Imbalance Based on Multiple Regression Analysis

The heat imbalance is observed in actual data, which is well known as a "closure issue" [3] [4]. Therefore, the data was corrected conventionally according to Allen's procedure by multiple regression analysis [5]:

$$Rn - G = A \times lE + B \times H . \quad (11)$$

Here: Rn, G, lE and H are described earlier. A, B are the regression coefficient for lE, H.

To guarantee the heat balance relationship, all sites used the corrected data. In addition, the correction is conducted using the daily basis.

2.1.5. Constraint to Improve the Underestimation of *lE*

To improve the under or overestimation of lE *i.e.*, over or underestimation of H, we set the following constant defined as Equation (12):

$$b = q(Ts) - \frac{q(Ts) - q(Tz)}{Ts - Tz} \times Ts \tag{12}$$

b is a constant passing through straight line at $T = 0^{\circ}\mathrm{C}$ with slope $\left[q(Ts) - q(Tz)\right] / (Ts - Tz)$. In Equation (12) the $q(Ts)$ and $q(Tz)$ are converted from $e(Ts)$ and $e(Tz)$ using $q(Ts)$ and $e(Ts)$ relationship.

The constraint for optimization process set as follows:

$$b \le 0 \quad \text{or} \quad b \ge 0\,. \tag{13}$$

The constraint is expected increasing of lE_{est}, whereas decrease H_{est} at high humidity area or vice versa. General analysis applied the constraint of Equation (13).

In addition, the constraints of Equation (13) have a similar role of $rehs > rehz$ or $rehs < rehz$ depending on initial values of $rehs = rehz$ or $rehs = 1.0$ that is expected in humid region.

2.1.6. Initial Values for Optimization and Constraints

The initial values of Ts and $rehs$ are key factors for obtaining reliable results. The value of Ts is chosen as T_0 because the T_0 is observed at near the soil surface. The initial value of $rehs$ chosen as $rehs = 1.0$ because humid region or $rehs = rehz$ depending on site specific conditions. Then, RTs was assumed to be 0, The RTs was automatically improved to satisfy the optimum value of Ts and $rehs$.

The ε has very small values on the order of 10^{-15} W·m^{-2} initially, because B_{app} nearly satisfies the heat balance relationship. Therefore, the objective function is multiplied by 10^{15}. To avoid abnormal fluctuation of H and lE, in the optimization process, constraints on those are set as less than $(Rn - G)$ as mentioned earlier. Additionally, B_{app} is constrained as $-100 < B_{app} < 100$ by referring to the actual data and optimization process [1]. The reason is described in the discussion section. We set the precision: =0.000001 and convergence: =0.0001 in Solver option.

2.2. Investigation Sites and Equipment

To examine the proposed method, six sites were chosen in humid regions having annual precipitation over 1000 mm (Table 1), including a site in Japan, three sites in the USA and two sites in Europe. Site2-Jap data in Japan were prepared by Tukuba University (2006) [6]. Three sites in USA data were prepared by AmeriFlux (Brooks Field Site 11 of US-Br3 [7], Konza Prairie of US-Kon [8], Goodwin Creek of US-Goo [9]). And two sites of Europe data prepared by European Fluxes Database Cluster (Vall dAlinya of ES-VDA [10] and Dripsey of IE-Dri] [11].

H was observed by eddy covariance at all sites (H_{obs}). lE was also observed by eddy covariance at five sites (lE_{obs}) excluding site2-Jap. The lE_{obs} at site2-Jap was estimated by imbalance ($lE_{imb} = Rn - G - H_{obs}$). Rn and G were observed at all sites. As shown in Table 2, the soil temperature T_0 was observed by thermometer at the depth of 2 ~ 5 cm.

2.3. Heat Balance Relationship of Observed Sites and Data Gap

Table 3 describes the accuracy and data gap of the observed data at the tested sites ex-

pressed in heat flux. The imbalance was observed at USA and European sites because directory observed lE by the eddy covariance. US-Kon, IE-Dri and ES-VPA has remarkable large imbalance of 18%, 31% and 19%. The imbalance is zero at the site2-Jap because no observed of lE.

Site2-Jap, US-Br3, IE-Dri and ES-VPA have relatively small data gap while US-Kon and US-Goo have remarkable. The time of having data gap is avoided in the analysis. The annual precipitation of the examined year is shown.

3. Result

The general solution determines two variables, *Ts* and *rehs*, using two equations simultaneously. Therefore, *Ts* and *rehs* can be uniquely determined mathematically. The initial value is set as aforementioned. Furthermore, the heat balance is not achieved instantaneously; it requires a few hours [5]. Thus, the hourly figure adjusts to a five-hour moving average.

3.1. Conversion of Observed Data (H_{obs} and lE_{obs}) into Corrected Data (H_{cor} and lE_{cor})

Observed data do not achieve the heat balance relationship, as shown in Table 3. To maintain the relationship, multiple regression analysis is applied using Equation (11). Figure 2 describes the relationship ($Rn - G$) versus ($H + lE$) of the original and corrected data in which the observed data are shown in the red circle while the corrected data are shown in the blue circle. The slope of the five tested sites increased and approached to 1.0. The regression coefficients described in Table 4 are A for H and B for lE. The observed data are corrected by these coefficients for all of the tested sites.

3.2. Comparison of the Hourly Change of the lE and H at all Sites

To confirm the validity, Figure 3 compares the hourly changes in lE_{obs} with lE_{est} and

Table 1. Features of the tested sites.

Site name/FLUXNET ID:	Tsukuba/Site2-Jap	Brooks Field Site 11/US-Br3	Konza Prairie/US-Kon	Goodwin Creek/US-Goo	Dripsey/IE-Dri	Vall dAlinya/ES-VDA
Country:	Japan	USA	USA	USA	Ireland	Spain
State/province:	Tsukuba University/Ibaraki Pref.	Iowa	Kansas	Mississippi	Corcaigh	Cataluna
Latitude (+N/−S):	36.1135	41.9747	39.0824	34.2547	51.9867	42.1522
Longitude (+E/−W):	140.0948	−93.6936	−96.5603	−89.8735	−8.7518	1.4485
Elevation:	29.0 m	314 m	443 m	87 m	186 m	1787
Vegetation (IGBP):	Grasslands	Croplands	Grasslands	Grasslands	Grasslands	Grasslands
Tower height:	30.5 m	5 m	-	4 m	-	-
Canopy height:	0.1 - 1.0 m	-	0.4 m	0.20 - 0.40 m	-	-
Data available	1999 1/1-12/31	2010 1/1-12/31	2009 1/1-12/31	2006 1/1-12-31	2008 1/1-12-31	2008 1/1-12-31

Table 2. Measurement instruments of the tested sites including D_{To}.

Site name/FLUXNET ID:			Tsukuba/Site2-Jap	Brooks Field Site 11/US-Br3	Konza Prairie/US-Kon	Goodwin Creek/US-Goo	Dripsey/IE-Dri	Vall dAlinya/ES-VDA
Variable	Units	Description	Model	Model	Model	Model	Model	Model
FG	$W \cdot m^{-2}$	Soil heat flux	Soil Heat Flux Plate (CPR-PHF-01, Cmimatec)	Soil Heat Flux Plate (HFT, REBS)	Soil Heat Flux Plate (HFT-3, REBS)	Soil Heat Flux Plate (HFP01SC, REBS)	Soil Heat flux plate (HFP01)	Soil Heat flux plate (HFP10SC, Hukseflux)
H	$W \cdot m^{-2}$	Sensible heat flux	Sonic Anemometer (DA-650, TR-61, AKAIJO SONIC Co.)	Sonic Anemometer (CSAT3, Campbell Scientific)	Sonic Anemometer (CSAT3, Campbell Scientific)	Sonic Anemometer (81,000 V, R. M. Young)	Sonic anemometer (CSAT, Campbell Scientific)	Sonic anemometer (R3A, Gill)
LE	$W \cdot m^{-2}$	Latent heat flux	-	Sonic Anemometer (CSAT3, Campbell Scientific) Open Path CO_2/H_2O Gas Analyzer (LI-7500, LI-COR)	Sonic Anemometer (CSAT3, Campbell Scientific) Infrared CO_2/H_2O Gas Analyzer (LI-6262, LI-COR)	Sonic Anemometer (81,001V, R. M. Young) Infrared CO_2/H_2O Gas Analyzer (Open-Path, ATDD/NOAA)	Sonic Anemometer (CSAT, Campbell Scientific) Open Path CO_2/H_2O Gas Analyzer (LI-7500, LI-COR)	Sonic Anemometer (R3A, Gill) Open Path CO_2/H_2O Gas Analyzer (LI-6262, LI-COR)
PREC	mm	Precipitation	Rain Gauge (WB0013-05, Yokogawa Denshikiki Co.)	-	-	Tipping Bucket Rain Gauge (TB3, Hydrological Services)	Rain gauge (arg100)	Precipitation Sensor (ARG 100, Environmental measurements Ltd)
PRESS	kPa	Barometric pressure	Barometric Pressure Sensor (PTB210, Vaisala)	-	-	Barometric Pressure Sensor (PTB101, Vaisala)	Barometric Pressure Sensor (PTB1001, Vaisala)	Sensor technics (model 144SC0811BARO)
RH	%	Relative humidity of air	Temperature/ Humidity Probe (CVS-HMP45D, Climatec)	Temperature/ Humidity Probe (HMP35, Vaisala)	Temperature/ Humidity Probe (HMP45C, Vaisala)	Temperature/ Humidity Probe (HMP50Y, Vaisala)	Temperature/ Humidity Probe (HMP45C, Vaisala)	Temperature & humidity transmitter (MP100, Rotronic)
Rn	$W \cdot m^{-2}$	Net radiation	Net Radiometer (CN-11, EKO Instruments)	Net Radiometer (Q*7.1, REBS)	Net Radiometer (Q*7.1, REBS)	Net Radiometer (Kipp-zonen, CNR1)	Net Radiometer (CNR1, Kipp-zonen)	Net Radiometer (CNR1, Kipp-zonen)
TA	deg C	Air temperature	Temperature/ Humidity Probe (CVS-HMP45D, Climatec)	Temperature/ Humidity Probe (HMP35, Vaisala)	Temperature/ Humidity Probe (HMP45C, Vaisala)	Temperature/ Humidity Probe (HMP50Y, Vaisala)	Temperature/ Humidity Probe (HMP45C, Vaisala)	Temperature & humidity transmitter (MP100, Rotronic)
T_0	deg C	Soil temperature	Soil temperature Probe (C-PTG-10, Climatec)	Thermocouple (Type T)	-	-	-	-
D_{To}	cm	Depth of measurement	2	2	2	2	2.5	5

Data store: every 30 minutes, hourly.

H_{obs} or H_{est} at the six sites in summer. All sites data are reproduced well.

However, in detail, lE_{est} is coincided very well with lE_{cor} excluding IE-Dri whereas H_{est} also very well coincided with H_{cor} without US-Kon. The small differences of H_{est} may have a little reflected to the lE_{est}. The other terms, such as lE_{obs} and H_{obs} describe almost similar trends but have small site specific differences. In addition, the initial values of

Table 3. Heat balance of the sites including data gap and annual precipitation (unit: heat flux).

Site name	Year	Period	Unit	Heat balance components ($W \cdot m^{-2}$)					Ra_{imb}	Data gap	Precipitation	Remarks
				Rn	*G*	*H*	*lE*	Imbalance	(%)	(%)	($mm \cdot year^{-1}$)	for *lE*
Site2-Jap	1999	1/1-12/31	$W \cdot m^{-2}$	28,584	−305	5229	23,659	0	0	8	1336	Heat balance
			$mm \cdot year^{-1}$	1009	−11	185	835	0				
US-Br3	2010	1/1-12/31	$W \cdot m^{-2}$	27,783	330	6286	19,385	1783	6	9	1392	Observed
			$mm \cdot year^{-1}$	981	12	222	684	63				
US-Kon	2009	1/1-12/31	$W \cdot m^{-2}$	30,344	−684	9220	16,603	5205	18	20	1054	Observed
			$mm \cdot year^{-1}$	1071	−24	325	586	184				
US-Goo	2006	1/1-12/31	$W \cdot m^{-2}$	32,948	1060	9662	19,402	2824	8	29	1369	Observed
			$mm \cdot year^{-1}$	1163	37	341	685	100				
IE-Dri	2008	1/1-12-31	$W \cdot m^{-2}$	28,241	−341	3039	14,893	8941	31	8	1308	Observed
			$mm \cdot year^{-1}$	616	−12	107	526	316				
ES-VDA	2008	1/1-12-31	$W \cdot m^{-2}$	21,922	330	5991	11,434	4168	19	2	1227	Observed
			$mm \cdot year^{-1}$	774	12	211	404	147				

Note: Data gap is not available data for analysis, *i.e.*, lacked one of which *G*, T_a, T_0, *P*, *erhz*, *Rn*, H_{obs} and lE_{obs}. Imbalance is estimated by $Imb = Rn - G - lE - H$ using yearly observed data and the imbalance ratio defined as $Ra_{imb} = Imb/(Rn - G)$. 100 $W \cdot m^{-2}$ = 3.53 $mm \cdot day^{-1}$ [12].

rehs set as follows: US-Kon and US-Goo are *rehs* = *rehz* with constrains $b < 0$ and the other sites uses *rehs* = 1.0 with constrains $b > 0$.

3.3. Annual Change of the Estimated and Observed *lE* and *H*

Figure 4 describes the yearly changes of the estimated and observed *lE* and *H* for the six sites. All sites describe that the trend relatively well reproduced. However in detail, the results show small differences at spring of lE_{est} at US-Kon. It shows overestimate for lE_{est} while shows underestimate for H_{est}. The other terms of lE_{obs} exhibits similar trends and H_{obs} also display the same trend but with small differences (not shown).

3.4. Comparison of the Observed and Estimated *lE* and *H*

Figure 5 compares the relationship of *lE* and *H* on daily basis to confirm the validity of the general solution. If the slope (slope of the straight line) is 1.0, the observed value coincides are well with the estimated values. For lE_{est}, all sites well reproduced (±15%) whereas lE_{est} are underestimated (>15%) excludes US-Goo. R^2 (R is corrected determination coefficient) of lE_{est} shows underestimated at US-Kon (>60%) and R^2 for H_{est} show remarkably small values excludes ES-VDA. In addition, the criteria of accuracy (±15%) were determined referring to observed data (Table 3).

3.5. Relationship of the *rehz* and T_0 and Estimated *rehs* and *Ts*

The relationship between estimated *rehs* and observed *rehz*, *i.e.*, the initial values, is a great concern to obtain the reliable results. The left hand side of Figure 6 shows hourly

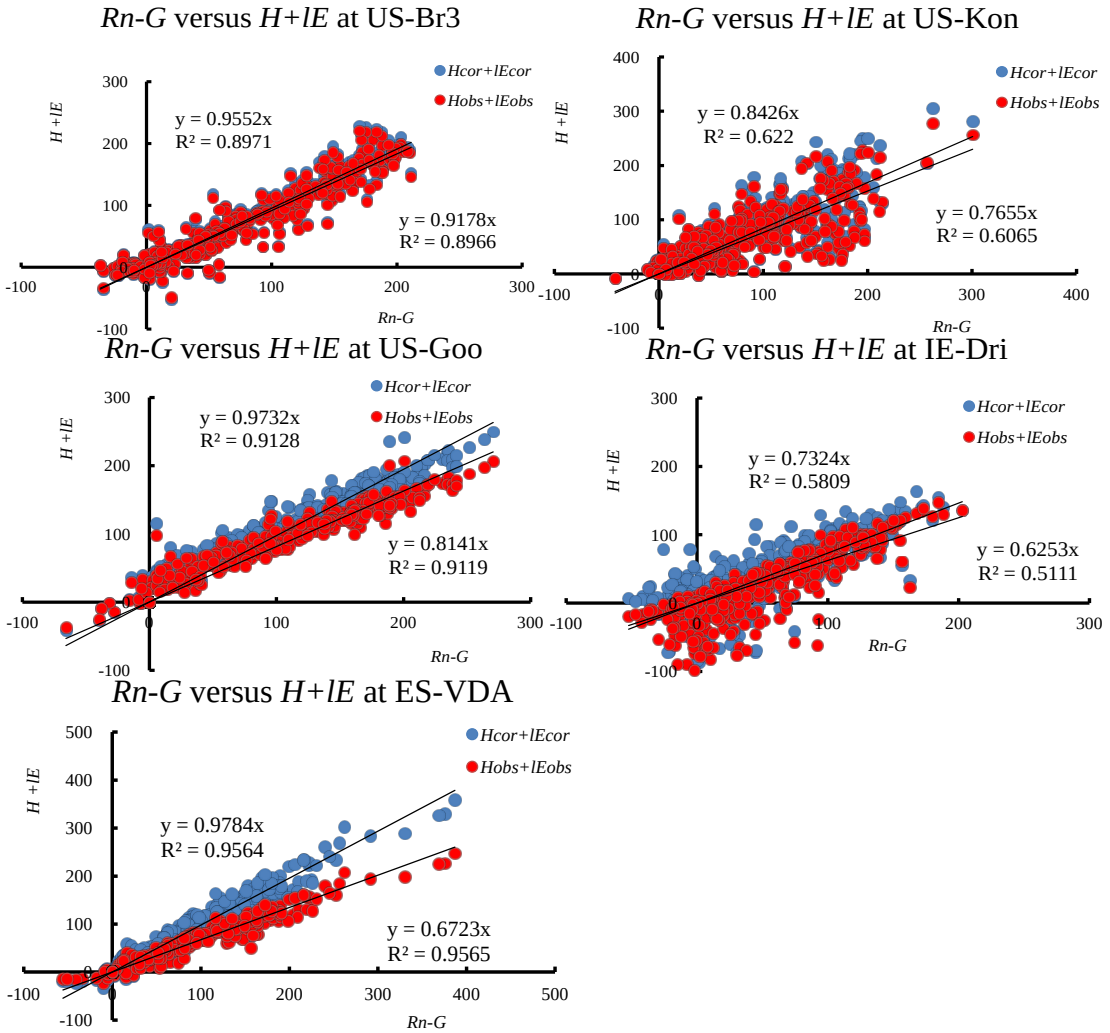

Figure 2. Comparison of ($Rn - G$) with ($H + lE$) observed and corrected (W·m^{-2}).

Table 4. Regression coefficient for lE and H.

Site Name	A	B	R^2
Site2-Jap	1.000	1.000	0.997
US-Br3	1.164	1.030	0.927
US-Kon	1.186	1.123	0.835
US-Goo	1.082	1.252	0.970
IE-Dri	1.135	1.496	0.916
ES-VDA	1.435	1.472	0.976
Average	1.167	1.229	0.937

A is regression coefficient for lE, B is regression coefficient for H.

change of *rehs* and *rehz* in summer. The figure describes the well functioned optimization process because the *rehs* changed remarkably from initial values of 100% of *rehz*. Difference of *rehs* and *rehz* is quite small at all sites. The right hand side of Figure 6

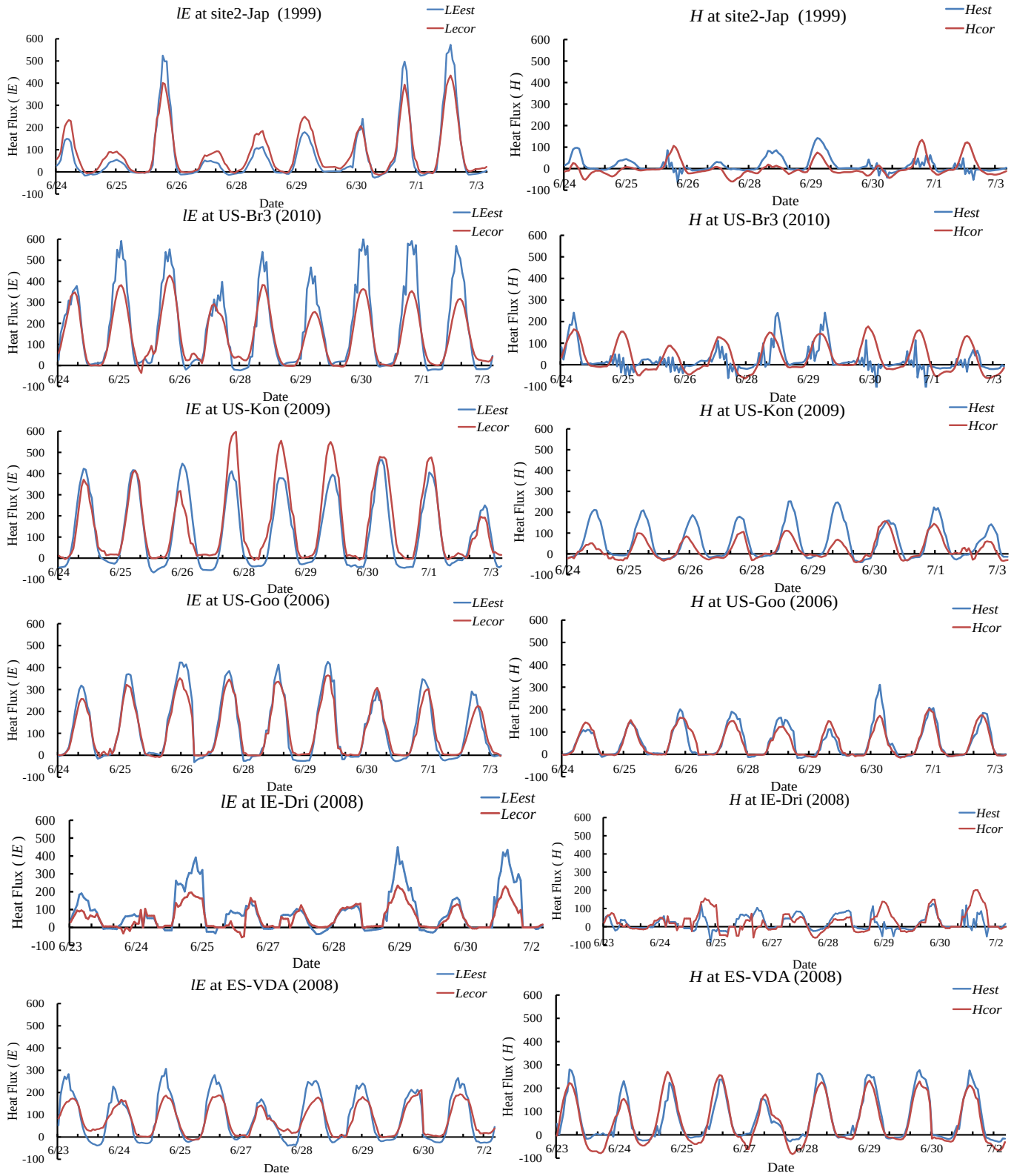

Figure 3. Hourly changes of *lE* and *H* observed and estimated (W·m^{-2}) (general solution). Note: 1) Initial condition at site2-Jap, US-Br3, IE-Dri and ES-VDA are *rehs* = 1.0. US-Kon and US-Goo are *rehs* = *rehz*. 2) Constraints: at site2-Jap, US-Br3, IE-Dri and ES-VDA are $b > 0$. US-Kon and US-Goo are $b < 0$.

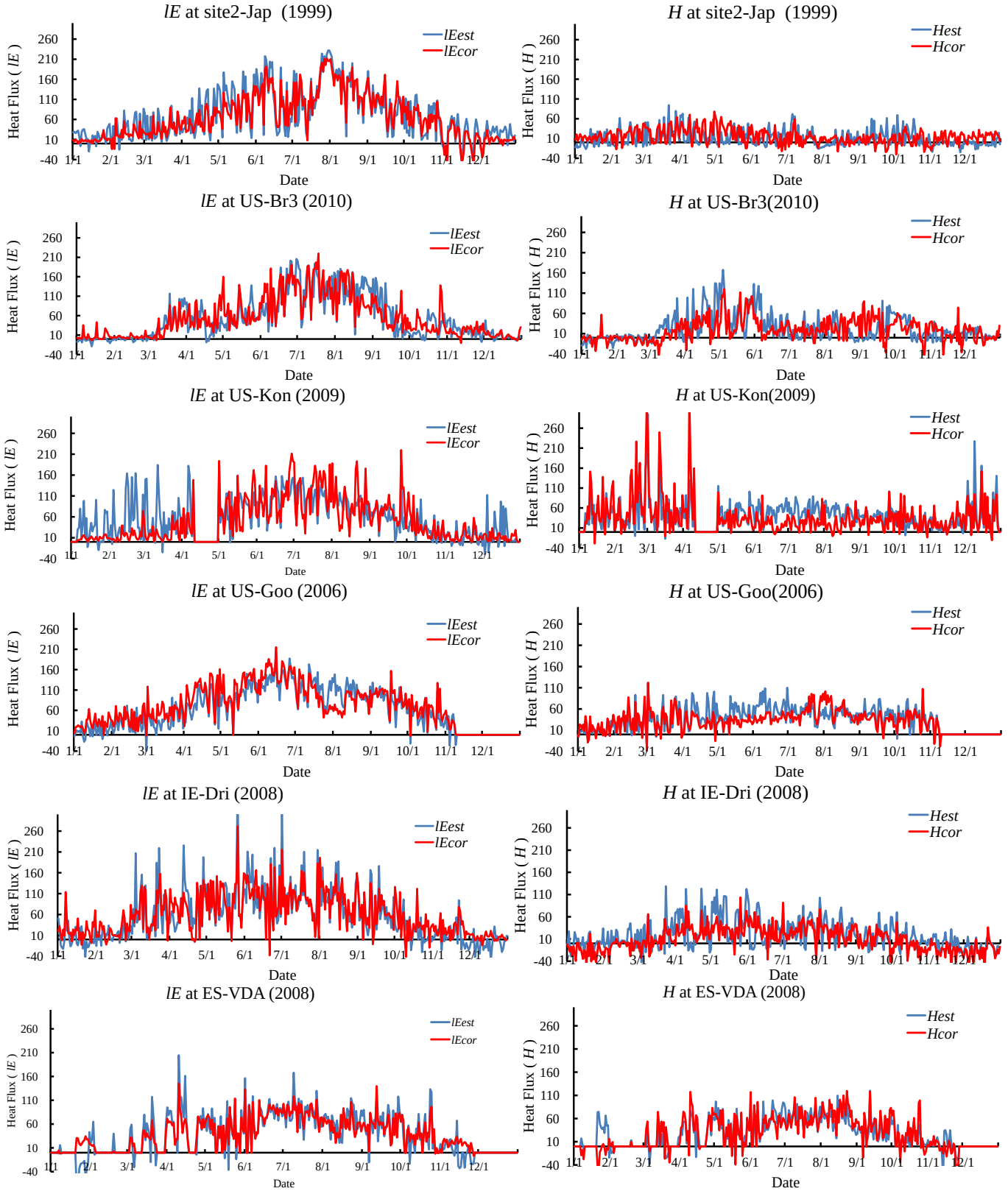

Figure 4. Yearly change of *lE* and *H* observed and estimated ($W \cdot m^{-2}$) (general solution). Note: Initial condition and constraints are the same with Figure 3.

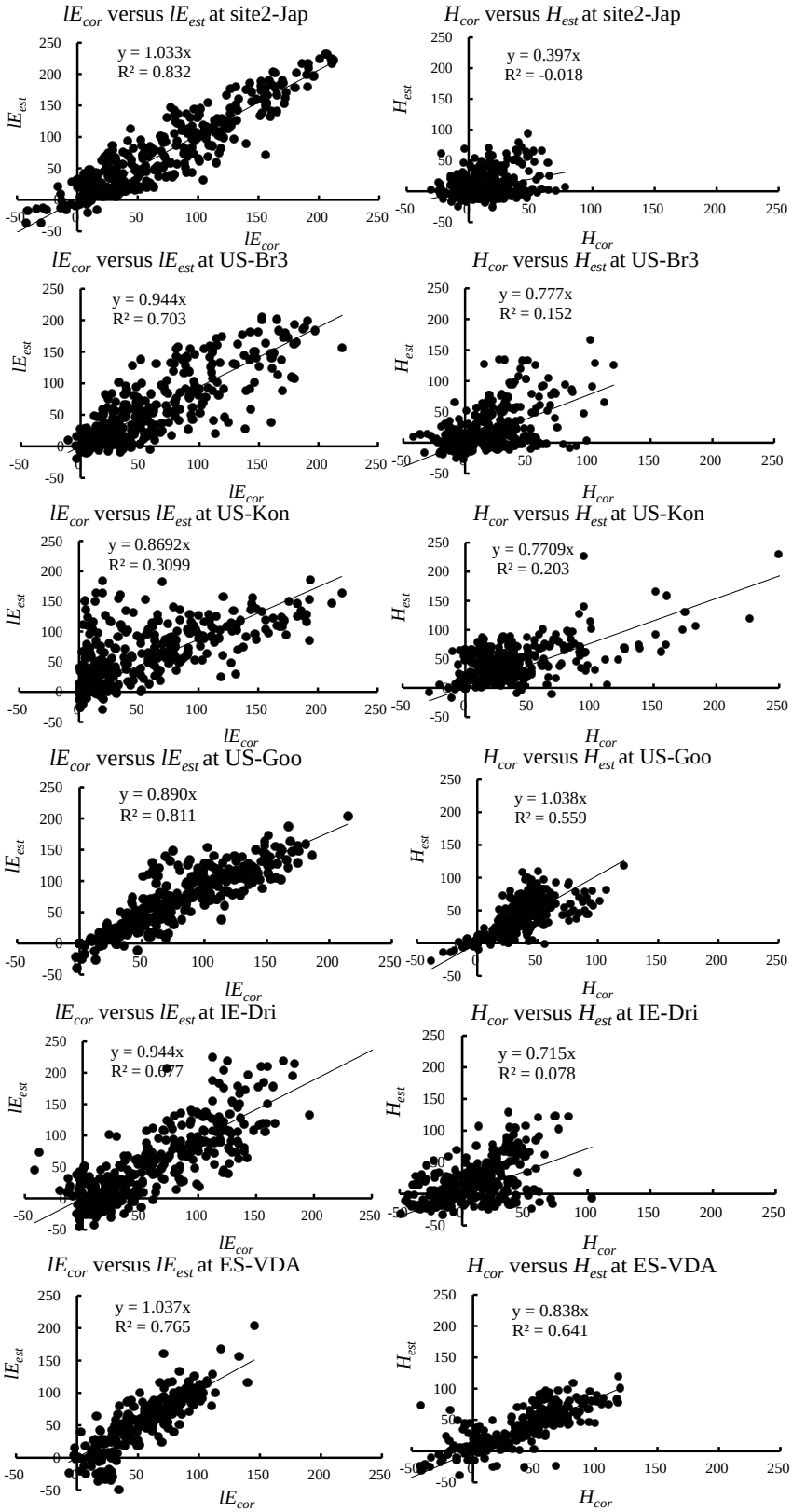

Figure 5. Comparison of *lE* and *H* observed and estimated (W·m^{-2}). Note: Initial condition and constraints are the same with **Figure 3**.

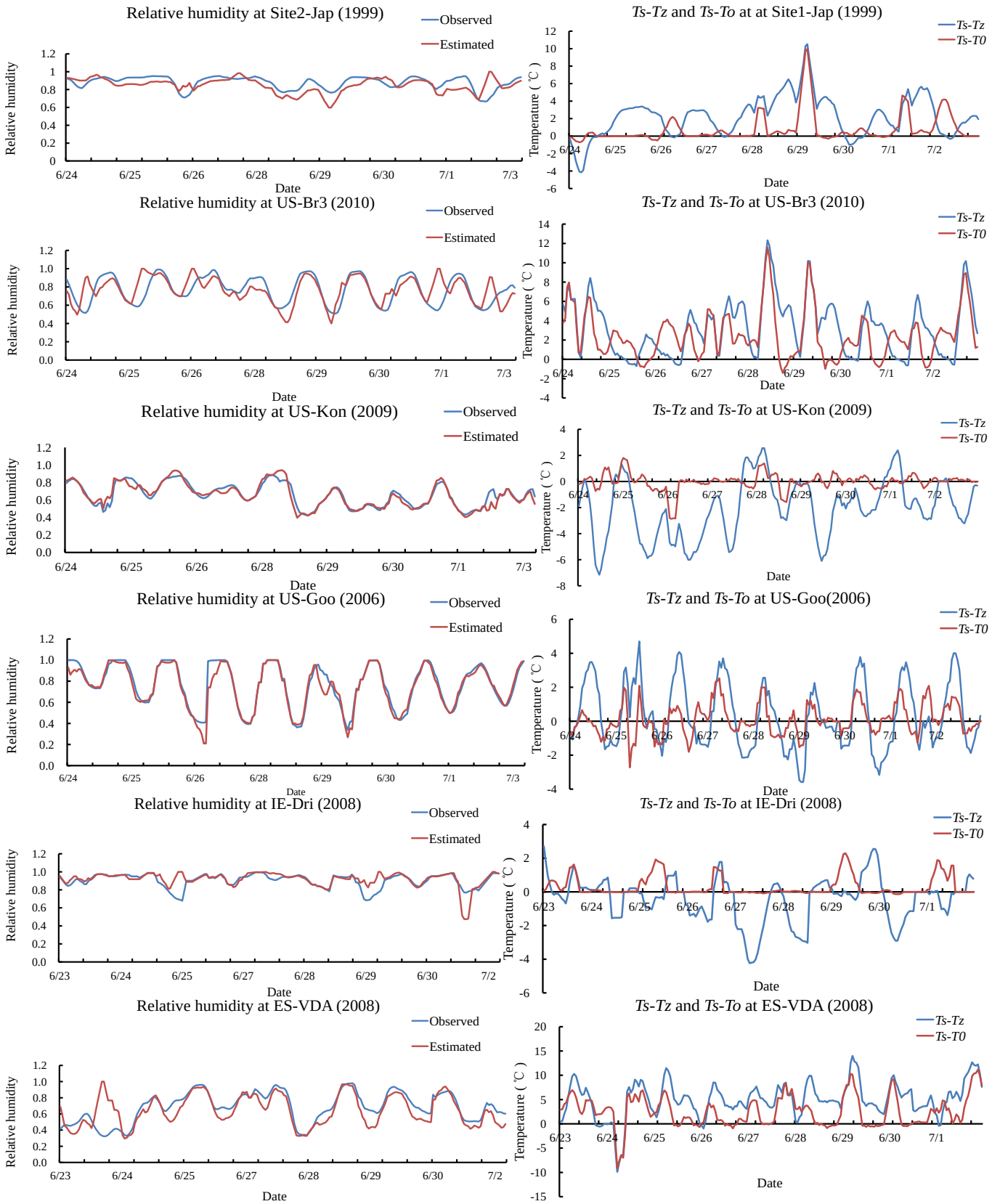

Figure 6. Hourly change of *rehs* and *Ts* (general solution). Note: Initial condition and constraints are the same with **Figure 3**.

shows the change of $Ts - T_0$ and $Ts - Tz$. The Ts changed remarkably from initial value T_0. The $Ts - T_0$ changes a difference ranging from −10˚C to +10˚C at site1-Jap and ES-VDA while −3˚C to +2˚C at US-Kon, US-Goo and IE-Dri, and from −3˚C to +12˚C at US-Br2. The difference Ts and Tz is about −10˚C to +12˚C, which has no site specific trends. The above features of *rehs* and Ts changes are quite similar to the other that in season although they have a small difference.

Seasonal change of the lE and H at the all sites is also investigated. The feature has not remarkable difference among February, May, Jun-July, September and November, although the quantity has season specific changes.

3.6. Slope of Estimated against Observed in All Analyzed Data

Table 5 describes all analyzed daily data at tested six sites including observed and corrected versus estimated using the proposed method for lE and H as well as Ts versus T_0 with *rehs* versus *rehz*. The feature is site specific. For corrected against estimated lE and H, the relationship is already described by Figure 5.

For lE_{obs} versus lE_{est}, IE-Dri and ES-VPA are overestimated (>15%). For H_{obs} versus H_{est}, US-Goo and ES-VPA are overestimated while the other sites are underestimated. (<±15%).

The Ts versus T_0 relationship are strongly correlated for all sites. The relationship of *rehs* versus *rehz* is also strong randomized at site-Jap and US-Br3, US-Kon remarkably

Table 5. All data analyzed by general method (general solution).

Site Name	item	lE_{cor}	H_{cor}	lE_{obs}	H_{obs}	$Ts \sim T_0$	*rehs* ~ *rehz*
Site2-Jap	Slope	*1.033	0.397	*1.033	0.397		1.079
	R^2	0.832	0.018	0.832	0.018		−1.500
US-Br3	Slope	*0.944	0.777	*0.966	0.848	1.121	1.070
	R^2	0.703	0.152	0.703	0.153	0.970	0.656
US-Kon	Slope	*0.869	0.771	*0.976	*0.914	0.997	0.917
	R^2	0.310	0.203	0.310	0.203	0.997	0.605
US-Goo	Slope	*0.890	*1.038	*1.114	1.222	1.013	0.957
	R^2	0.811	0.559	0.811	0.559	0.951	0.953
IE-Dri	Slope	*0.944	0.715	1.407	0.823	1.028	1.045
	R^2	0.677	0.078	0.677	0.078	0.961	0.768
ES-VDA	Slope	*1.037	0.838	1.383	1.231	1.135	1.075
	R^2	0.765	0.641	0.765	0.641	0.982	0.914
Average	Slope	0.953	0.756	1.146	0.906	0.882	
	R^2	0.683	0.275	0.683	0.275	0.810	

Slope express the gradient of estimation (lE_{est}, H_{est}) against correction (lE_{cor}, H_{cor}) and observation (lE_{obs}, H_{obs}), Initial condition *rehs* = *rehz*, $b > 0$. Note * indicates ±15%. Note: initial cindition at site2-Jap, US-Br3, IE-Dri and ES-VDA are *rehs* = 1.0. US-Kon and US-Goo are *rehs* = *rehz*. Constraints: at site2-Jap, US-Br3, IE-Dri and ES-VDA are $b > 0$. US-Kon and US-Goo are $b < 0$.

randomized.

3.7. Comparison of Estimated and Observed Evapotranspiration Rate (*ETa*)

Using observed and estimated *lE*, monthly evapotranspiration was obtained at the all sites, as shown in Figure 7 by assuming 100 $W \cdot m^{-2}$ equivalents for 3.53 $mm \cdot day^{-1}$ [12]. The initial value of *rehs* and constrains are chosen as aforementioned. If there are data gap in a given month, the monthly average *ETa* obtained as follows: The average *ETa* in a day multiplied the number of days of the month.

All sites describe very well reproduced the monthly change of *ETa.* In detail, although there are small differences between ETa_{obs}, ETa_{cor}, and ETa_{est} at all sites, the difference was relatively small.

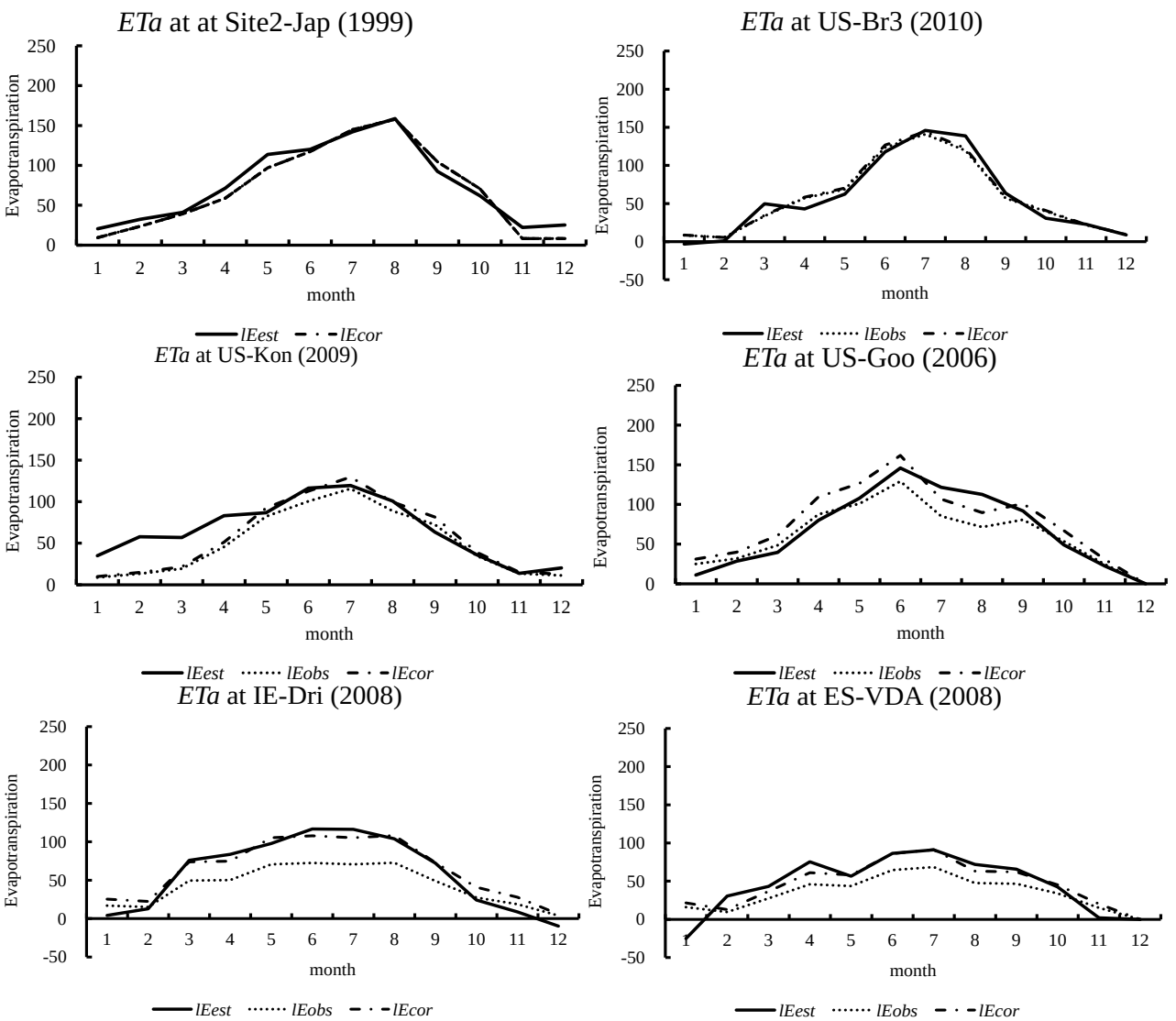

Figure 7. Comparison of observed (ETa_{obs}) and estimated (ETa_{est}) monthly evapotranspiration ($mm \cdot month^{-1}$). Note: Initial condition and constraints are the same with Figure 3. Observed data attached as reference.

Besides the pattern of monthly changes, the total amount of the *ETa* is summarized in Table 6. The amount of annual lE_{est} and H_{est} are satisfactorily consistent with lE_{cor} and H_{cor} or lE_{obs} and H_{obs}, *i.e.*, ETa_{est}/ETa_{cor} (<±15%) excluding US-Kon. US-Kon has big imbalance 140 mm·year^{-1} even if after correction by regression analysis. The other sites have a relatively small imbalance. The facts describe that *ETa* can be estimate by our method within 85% accuracy.

4. Consideration

4.1. Relationship of Penman Method with Proposed Method

To verify the validity of our method, our method was compared with penman method. Penman method is used to evaluate evaporation from the saturated or wet soil surface that corresponding to our proposed method as *rehs* equals to 100%.

Penman evaporation evaluated by Equation (14) [13]

$$Ep = \frac{\Delta}{\Delta+\gamma}\times\frac{Rn}{\lambda}+\frac{\Delta}{\Delta+\gamma}\times 0.26\times\left(1+0.537\times U_{10}\right)\times\left\{e_{sat}\left(Tz\right)-e\left(Tz\right)\right\}. \quad (14)$$

Here, Δ is the slope of saturated vapor pressure curve (hP·˚C^{-1}) at Tz, γ is hygroscopic constant (hP·˚C^{-1}), λ is latent heat flux (MJ·kg^{-1}), U_{10} is wind speed at 10 m height (m·sec^{-1}), another variable already described.

Figure 8 describes the comparison of evaporation estimated by Penman method with our proposed method using daily data of Ishikawa Prefectural Forest Experimental Station (Latitude (+N/−S): 36.4309, Longitude (+E/−W): 136.6424) (2014). The result by our method obtained using Equation (3) that optimized *Ts* at 100% of *rehs* reproduced well Penman's result even though a little scattered. The scattered point may produce with observation quality by related climate elements. Our method does not require the wind speed correction that appeared in the second term of right hand side in Penman Equation (14), which was already pointed out by Urano [13]. In addition, constraint of $Rn - G > lE$ and H is applied.

Table 6. Total amount of evapotranspiration estimated and observed including correction (mm·year^{-1}).

Site name	*Hest*	*lEest*	*Hcor*	*lEcor*	*Hobs*	*lEobs*	lE_{est}/lE_{cor}	H_{est}/H_{cor}	Imbalance
Site2-Jap	126	901	188	839	188	839	*1.07	0.67	0
US-Br3	287	681	241	702	221	686	*0.97	1.19	26
US-Kon	589	789	558	680	470	606	1.16	*1.06	140
US-Goo	472	810	410	925	379	739	*0.88	*1.15	−52
IE-Dri	241	706	110	770	96	517	*0.92	2.19	67
ES-VDA	384	540	377	559	257	419	*0.97	*1.02	−11

Note 1) Initial cindition at site2-Jap, US-Br3, IE-Dri and ES-VDA are *rehs* = 1.0. US-Kon and US-Goo are *rehs* = *rehz*. 2) Constraints: at site2-Jap, US-Br3, IE-Dri and ES-VDA are $b > 0$. US-Kon and US-Goo are $b < 0$. 3. Imbalance: $(H_{est} + lE_{est}) - (H_{cor} + H_{obs})$. Note * indicates ±15%.

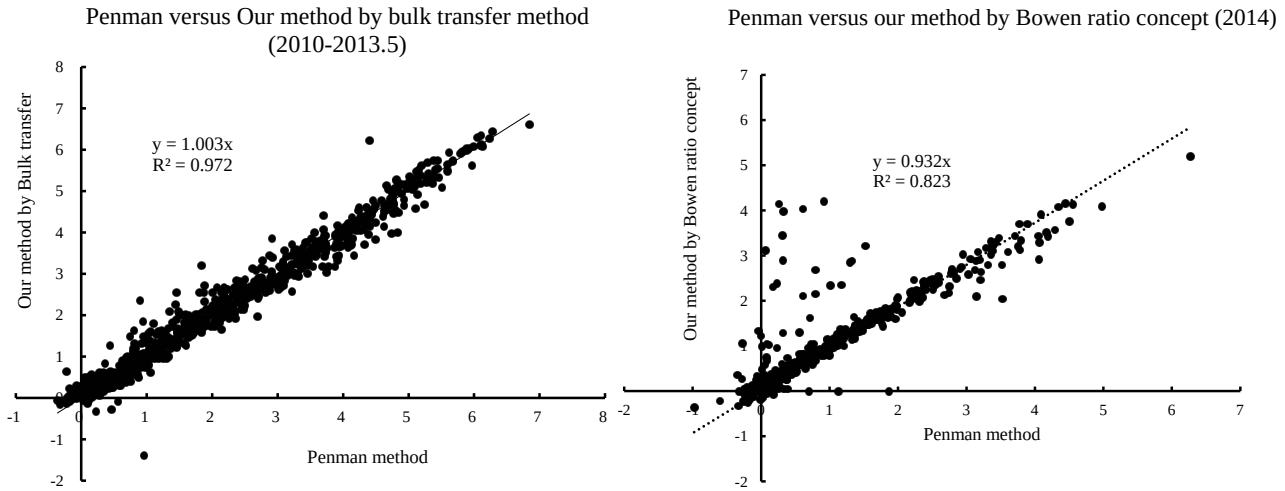

Figure 8. Comparison of Penman method with our method ($W \cdot m^{-2}$).

4.2. Comparison of Bulk Transfer Method at Wetted Soil Surface with our Method

Furthermore, to obtain more reasonable result, we applied the Bulk Transfer Concept (BTC). The heat balance equation of the BTC can be expressed as Equation (15) [14]. The third term of left hand of the equation expressed the sensible heat flux and the fourth term expressed the latent heat flux. Before optimization, Equation (15) is not closed because C_H, C_E and Ts are assumed. The optimization conducted as the ε goes to minimum.

$$Rn - G - \rho C_P C_H (Ts - Tz) Uz - l\rho C_E \left(\frac{0.622}{P}\right)\left[e(Ts) - e(z)\right] Uz = \varepsilon . \qquad (15)$$

Here, C_H is bulk transfer coefficient of sensible heat flux, C_E is bulk transfer coefficient of latent heat flux, Uz is wind speed, other variables already described.

As described in **Figure 8**, our method using Equation (15) with the condition of $C_H = C_E$, that is the same of Penman method's assumption [14], is very well reproduced, although the procedure does not unified the variables $C_H = C_E$ and Ts mathematically because one equation determine two variables.

4.3. Comparison of Observed *Ts* with Estimated by Radiometer *Ts*

To verify the reasonability of estimated *Ts*, **Figure 9** compares the estimated *Ts* with observed *Ts* by radiometer at three sites. The sites almost indicate well coincident with each other, thus, the data shows the validity of the *Ts* estimation.

5. Discussion

5.1. Initial Values and Constraints

There are plural results *i.e.*, local minimum, as satisfying Equation (8) and Equation (9) at different initial values because of nonlinear simultaneous solution. One of the technical points of our research is how to find out the reasonable initial values of *Ts* and

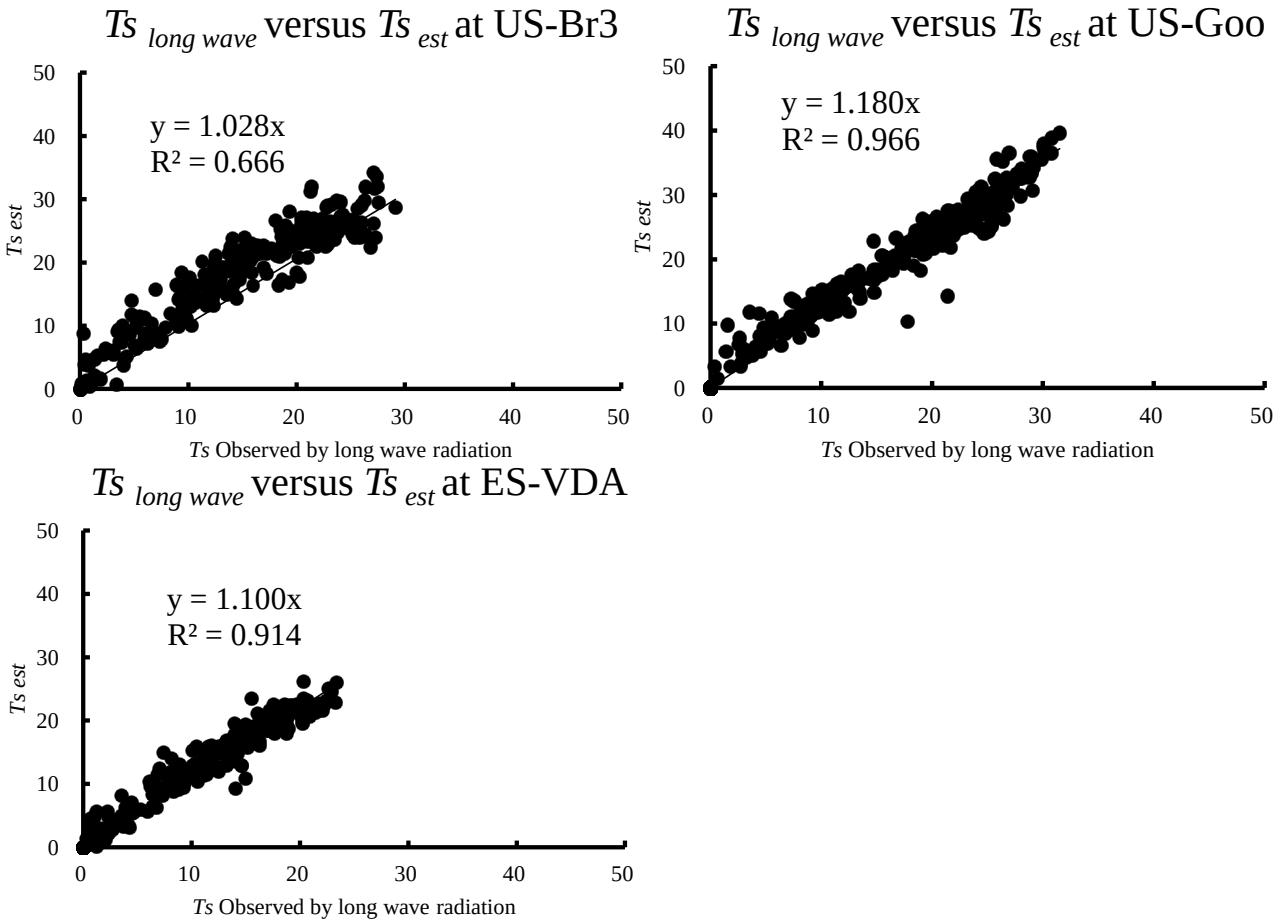

Figure 9. Comparison of *Ts* observed by radiometer and estimated (˚C).

rehs with constrains. We approach the final values of *rehs* and *Ts* from both sides saturated and observed *rehz* with constraints of $b < 0$ or $b > 0$. The results obtained by this procedure are mostly successful. One important thing is that the initial values *Ts* and *rehs* to be set as possible as vicinity to the final values.

5.2. Abnormal Fluctuation of B_{app} (Singularity of B_{app})

If *Ts* approaches zero in convergence process, B_{app} is remarkably increased according to approaching zero from the opposite side, positive and negative, as shown in **Figure 10**. This tendency is almost independent of $(Ts - Tz)$, although there are small differences. Actually, when denominator of Equation (4) approaches zero $\left[q\left(T_{s,ass}\right) = q\left(T_z\right)\right]$ *i.e.*, *rehs* approaches to $rehz \times \left[q_{sat}\left(Tz\right) \cdot q_{sat}\left(Ts\right)^{-1}\right]$, the abnormal B_{app} appeared. To avoid this conflict, B_{app} is limited to $(-100 < B_{app} < 100)$ as aforementioned, referring to the observed and calculated data approximately [1].

6. Conclusions

In the natural world, the air temperature and humidity reflect the partitioning of sensible and latent heat flux from *Rn* and *G*. Based on this concept, we attempt to estimate *H*

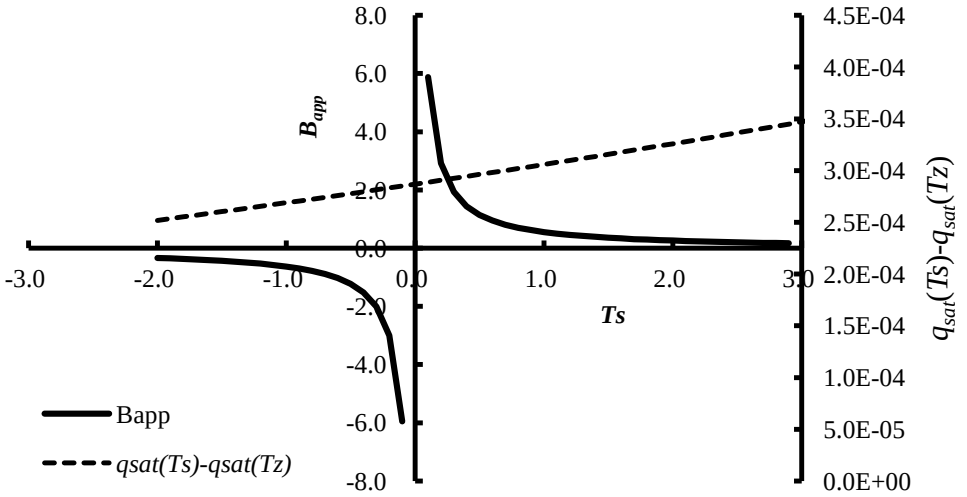

Figure 10. Relationship between B_{app} and temperature Ts when $Ts - Tz = 1.0^{\circ}\mathrm{C}$ [1].

and lE reciprocally using single height temperature and humidity, and Rn and G by applying the Bowen ratio concept on the soil surface. This feature can be remarkably extended to the field of utilization. The unknown variables Ts and $q(Ts)$ (*i.e.*, *rehs*) are estimated by an optimization procedure as satisfying heat balance relationship. The validation of the method was achieved by the six sites in the humid regions of Japan, USA and Europe. lE and H were observed by the eddy covariance method at these sites, except lE in Japan site. Analysis is conducted on an hourly basis and summarized daily. The main results are as follows:

1) The hourly and yearly change of the estimated lE and H very well coincided with the observed values at all sites.

2) The estimated lE and H versus corrected lE and H or observed lE and H are satisfactory coincided.

3) The hourly change of Ts and *rehs* can be estimated by the method that is very difficult to observe at actual site.

4) The estimated evaporation ETa satisfactorily coincided with corrected and observed ETa not only monthly change but also annual amount.

5) The method compared with penman method and confirmed the validity.

The estimated results have not completely reproduced the observations, but the results are mostly satisfactory. This fact shows that the method is useful for the estimation of lE and H. The remarkable feature of the new method is that it is applicable for the approximate of lE and H using a single height of Tz and *rehz* with Rn and G. For estimation of ETa, this method will be applicable to various local areas because of required data easily obtained.

But, there are problems that still remain. The error plain *i.e.*, ε_i in Equation (3) related to Ts and *rehs*, is very complicated because of nonlinear simultaneous equation having many local minimum. Therefore, the selection of initial values of Ts and *rehs* is important issue to be solved in future. On the other hand, this research is restricted at humid region but analysis of sensible and latent heat flux at arid and semi-arid region is

also very important. This is also another big problem to be solved in future.

We conclude that the partitioning of *lE* and *H* is controlled by energy conservation in nature. Realistically, the observed temperature and humidity are strongly affected by the partitioning of *H* and *lE*, and vice versa. Therefore, using the observed temperature, humidity and common climate elements, the *lE* and *H* values are reciprocally approximated by the optimized techniques.

Acknowledgements

We sincerely thanks for providing the AmeriFlux and EuroFlux principal investigation for data accessed on July 5, 2015. We sincerely thank Dr. Asanuma Jun, a professor at Tsukuba University, for providing valuable data for the eddy covariance method; Dr. Kuwagata Tsuneo, Dr. Fujihara Yoichi and Dr. Takimoto Hiroshi for providing valuable comments on the optimization procedure. We also thank Dr. Yoshida Masashi and Dr. Noto Fumikazu, who are staff members at Ishikawa Prefectural University, for recording the data. We also thank the staff at the Ishikawa Forest Experiment Station.

References

[1] Maruyama, T. and Segawa, M. (2016) Reciprocal Analysis of Sensible and Latent Heat Fluxes in a Forest Region Using Single Height Temperature and Humidity Based on the Bowen Ratio Concept. *Journal of Water Resource and Protection*, **8**, 724-742. http://dx.doi.org/10.4236/jwarp.2016.87059

[2] Kondo, J. (1996) Meteorology on Water Environment, 6. Water and Heat Balance on Soil Surface. Asakura Publishing Ltd., Tokyo, 128-159.

[3] Twine, T.E., Kustas, W.P., Norman, J.M., Cook, D.R., Houser, P.R., Meyers, T.P., Prueger, J.H., Staks, P.J. and Wesely, M.L. (2000) Correcting Eddy-Covariance Flux under Estimates over a Grassland. *Agricultural and Forest Meteorology*, **103**, 279-300. http://dx.doi.org/10.1016/S0168-1923(00)00123-4

[4] Wison, K., Goldstein, A., Falge, E., Abbinet, M., Baldocchi, D., Berbingier, C., Ceulemans, R., Dolman, H., Field, C., Grelle, A., Ibrom, A., Law, B., Kowalski, A., Meyers, T., Moncrieff, J., Monson, R., Oechel, W., Tenhunen, J., Valentini, R. and Verma, S. (2002) Energy Balance Closure at FLUXNET Sites. *Agricultural and Forest Meteorology*, **113**, 223-243.

[5] Allen, R. (2008) Quality Assessment of Weather Data and Micrometeorological Flux Impact on Evapotranspiration Calculation. *Journal of Agricultural Meteorology*, **64**, 191-204. http://dx.doi.org/10.2480/agrmet.64.4.5

[6] Asanuma, J. (2012) Site2-Jap, Data of Heat and Water Balance Observation, 1999-2011 by CD. Center for Research in Isotope and Environmental Dynamics, Tsukuba University.

[7] Prueger, J.H. (2010) Brooks Field Site 11 (US-Br3) AmeriFlux L2 Data. http://cdiac.esd.ornl.gov/programs/ameriflux/data_system/aaBrooks_Field_Site_11_pf.html

[8] Brunsell, N. (2009) Konza Prairie (US-KON) AmeriFlux L2 Data. http://cdiac.esd.ornl.gov/programs/ameriflux/data_system/aaKonza_Prairie_pf.html

[9] Meyers, T. P. (2006) Goodwin Creek (US-Goo) AmeriFlux L2 Data. http://cdiac.esd.ornl.gov/programs/ameriflux/data_system/aaGoodwin_Creek_pf.html

[10] Carrara, A. and Gimeno, C. (2008) Vall dAlinya (ES-VDA) European Fluxes Database Cluster L2 Data.

[11] Kiely, G., Leahy, P. and Foley, N. (2008) Dripsey (IE-Dri) European Fluxes Database Clus-

ter L2 Data.

[12] Kondo, J. (2015) Heat Balance and Climate on Soil Surface.

[13] Urano, S.-I. (2012) Study on Bowen ratios in the Penman and Priestly·Taylor Equations. *Geophysical Bulletin of Hokkaido University*, *Sapporo*, **15**, 91-107

[14] Kondo, J. (1996b) Meteorology on Water Environment, 5. Wind and Its Turbulence near Soil Surface. Asakura Publishing Ltd., Tokyo, 99-127.

Appendix 1

The GRG Nonlinear Solving Method for nonlinear optimization: developed by Leon Lasdon (University of Texas at Austin) and Alan Waren (Cleveland State University) and enhanced by Frontline Systems, Inc.

For more information about the other solution algorithms, advice on building effective solver models, and solving larger scale problems, contact: Frontline Systems, Inc.

Web site: http://www.solver.com, E-mail: info@solver.com

Estimated results have not completely reproduced the observations, but the results are mostly satisfaction.

Appendix 2

Using modules of Visual Basic for Applications (VBA) in the manuscript

```
Sub Macro “Number1 ()
' Macro ”Number 1”：GRG method
  Dim r As Long
Dim lastRow As Long
  lastRow = Range(“〈Column Alphabet〉” & Rows Count).End (xlUp).Row
  SolverReset
  For r = 〈Start row number〉 To 〈End row number〉
  SolverReset
  SolverOptions Precision:=0.000001, Convergence:=0.0001, StepThru:=False, Scaling:=False _
, AssumeNonNeg:=False, Derivatives:=2
SolverOk SetCell:= "Row" & r, MaxMinVal:=2, ValueOf:=0_
, ByChange:=Range(Cells(r, 〈First column number〉), Cells(r, 〈Last column number〉))
SolverAdd CellRef:="$ 〈rehs's Column Alphabet〉" & r, Relation:=1, FormulaText:=1
SolverAdd CellRef:="$ 〈rehs's Column Alphabet〉" & r, Relation:=3, FormulaText:=0
SolverAdd CellRef:="$〈RTs's Column Alphabet〉" & r, Relation:=1, FormulaText:=5
SolverAdd CellRef:="$ 〈RTs's Column Alphabet〉" & r, Relation:=3, FormulaText:=－5
SolverAdd CellRef:="$ 〈H estimated's Column Alphabet〉" & r, Relation:=1, FormulaText:= "$ 〈Rn-G observed' s Column Alphabet〉$ &r
SolverAdd CellRef:="$ 〈H estimated's Column Alphabet〉" & r, Relation:=3, FormulaText:=－100
SolverAdd CellRef:="$ 〈LE estimated's Column Alphabet〉" & r, Relation:=1, FormulaText:= "$ 〈Rn-G observed' s Column Alphabet〉$ &r
SolverAdd CellRef:="$ 〈LE estimated's Column Alphabet〉" & r, Relation:=3, FormulaText:=－100
SolverAdd CellRef:="$ 〈B_app's Column Alphabet〉" & r, Relation:=1, Formula-
```

```
Text:=100
  SolverAdd CellRef:="$ 〈B_app's Column Alphabet〉" & r, Relation:=3, FormulaText:=
－100
  ※in case of b>0
  SolverAdd CellRef:="$ 〈b estimated's Column Alphabet〉" & r, Relation:=3, For-
mulaText:=0
  ※in case of b<0
  SolverAdd CellRef:="$ 〈b estimated's Column Alphabet〉" & r, Relation:=1, For-
mulaText:=0
  SolverSolve UserFinish:= True, ShowRef:="DummyMacro"
   Next
  End Sub
```